Semnan University

Journal of Modeling & Simulation in Electrical & Electronics Engineering (MSEEE)

Journal homepage: **https://mseee.semnan.ac.ir/journal/about /**

ISSN: 2821-0786

Improving the Performance of the RI Sensor Based on a Disk-shaped Graphene Absorber using Pyramidal Air Holes in the Dielectric Layer

Seyed Amin Khatami[1], Pejman Rezaei [1•], Mohammad Danaie[1]

Abstract-This manuscript introduces a highly sensitive refractive index sensor that utilizes a disk-shaped graphene absorber. This design takes advantage of graphene's exceptional properties and integrates pyramid-shaped air holes within the dielectric layer. The sensor operates in the terahertz (THz), with a specific focus on improving sensitivity and overall performance. Graphene's high electrical conductivity and tunable properties make it an ideal material for THz absorption, enabling precise detection of refractive index changes the proposed structure comprises a graphene pattern on the top layer, a SiO2 as dielectric in the middle layer, and a gold reflective in the bottom layer. Through full-wave simulation and transmission line modeling, the sensor's performance is validated, showing a remarkable rate of absorption of 99.99% at 4.26 THz. Further enhancement is achieved by introducing pyramidal air holes in the dielectric layer, significantly improving the sensor's quality factor and sensitivity. The quality factor of the sensor is improved from 14 to 23 by adding pyramidal air holes in the substrate layer. The structure was full-wave simulated using software CST with the FDTD solution method, and the transmission line method was done with the Matlab software. The results suggest that the planned sensor serves as a highly suitable candidate for early disease detection, including cancer and influenza, with potential applications in the medical industry.

***Index Term*: Air Holes; Graphene-based Absorber; Sensitivity; Refractive Index Sensor; Biomedical Sensing; Terahertz.**

I. INTRODUCTION

Terahertz (THz) frequencies, spanning from 0.1 to 10 THz, fall within the electromagnetic spectrum between the microwave and infrared regions. These frequencies offer a broad range of applications across various fields. In telecommunications, THz waves enable ultra-high-speed data transfer and next-generation wireless communication systems. In medical imaging, THz waves are non-ionizing and can penetrate biological tissues, making them ideal for detecting skin cancers and other abnormalities. Of course, it is also necessary to mention that in the GHz frequency range, countless works have been done in the field of sensing and similar works in the terahertz range. THz spectroscopy is used in chemistry and materials science for identifying molecular compositions. Additionally, THz technology plays a significant role in security screening, allowing for the detection of concealed weapons and explosives. Its applications in astrophysics and environmental monitoring are also expanding, providing insights into cosmic phenomena and atmospheric pollutants [1-5]. THz absorbers are devices or materials designed to absorb THz radiation, typically in the 0.1 to 10 THz frequency range [6-10]. These absorbers are crucial for different applications, such as controlling THz waves in imaging, sensing, and communications. In security and stealth technologies, THz absorbers reduce the reflection of radiation, making them useful for cloaking and minimizing detection. In imaging systems, they help reduce noise and improve signal clarity. Materials like metamaterials, graphene, and dielectric composites are commonly used to design efficient THz absorbers, which are tailored for high absorption efficiency and bandwidth. THz absorbers also find applications in electronics, as they can prevent unwanted THz interference in devices, ensuring better signal transmission and reception [11-16].

Graphene, composed of a monolayer of carbon atoms

[1] Electrical and Computer Engineering Faculty, Semnan University, Semnan, Iran.
• Corresponding author Email: prezaei@semnan.ac.ir

Cite this article as:
Khatami, A. and Rezaei, P., 2024. Improving the Performance of the RI Sensor Based on a Disk-shaped Graphene Absorber using Pyramidal Air Holes in the Dielectric Layer. Journal of Modeling & Simulation in Electrical & Electronics Engineering (MSEEE), 4(4), pp. 1-8.

https://doi.org/10.22075/mseee.2025.35330.1176

organized in a hexagonal shape, possesses remarkable thermal, electrical, and mechanical characteristics, positioning it as a groundbreaking material in nanotechnology. In THz applications, graphene is particularly valuable due to its tunable electronic properties and high carrier mobility [17-18]. Graphene-based THz absorbers are optimized to absorb THz radiation with high efficiency, leveraging graphene's ability to interact strongly with electromagnetic waves. These absorbers can be designed to achieve high absorption across a broad frequency range, making them well-suited for applications in THz imaging, sensing, and stealth technology. By adjusting the chemical potential or applying external fields, the absorption properties of graphene can be dynamically controlled, offering versatility in designing adaptive THz devices. Additionally, graphene's compatibility with flexible substrates allows for the development of lightweight, flexible THz absorbers, further expanding their potential applications in wearable electronics and communication systems [19-28].

A refractive index sensor incorporating a graphene-based THz absorber is a sophisticated device engineered to detect variations in its surrounding medium refractive index, utilizing the distinctive properties of graphene. In such sensors, graphene's high sensitivity to its environment allows for precise detection of shifts in the refractive index, which in turn affects the absorption characteristics at THz frequencies.

The graphene-based absorber amplifies the interaction between the incoming THz radiation and the medium, resulting in detectable shifts in the absorption spectrum as the refractive index changes. These sensors exhibit exceptional sensitivity, allowing them to detect tiny variations in the refractive index, making them valuable for applications in chemical and biological sensing, environmental monitoring, and material characterization. The tunable nature of graphene allows for the optimization of the sensor's performance across different THz frequency ranges, providing versatility and adaptability for a range of sensing applications. Additionally, the integration of graphene with other nanomaterials can further enhance the sensor's sensitivity and selectivity, paving the way for next-generation THz sensing technologies [29-37]. Alizadeh and colleagues present a graphene-based refractive index sensor that operates in the THz frequency range [29]. The sensor is engineered to detect and measure changes in the refractive index of substances, which is a critical property for identifying biomolecules and materials in bio-sensing applications. The study in [30] investigates the design and performance of a graphene-based refractive index sensor that incorporates a double split ring resonator (DSRR) metasurface to achieve high sensitivity. The work aims to enhance the precision of optical sensing, particularly for applications in material detection and bio-sensing. Nickpay and colleagues contribute to the field of sensing technology by introducing a graphene-based, multi-band MPA that operates in the THz frequency range [31]. It combines the strengths of graphene and metamaterials to achieve high sensitivity and versatility in refractive index sensing, with applications in bio-sensing, chemical detection, and material analysis. This work represents a significant advancement in the development of efficient and practical THz sensors. The advancement of THz sensing by presenting a graphene disk-based refractive index sensor that is highly tunable and efficient for both TE and TM polarization modes introduced in [32]. The combination of tunability, high sensitivity, and dual-mode operation makes this sensor a promising tool for applications in bio-sensing, chemical analysis, and material characterization. In [33] presents a significant advancement in biosensing technology for the detection of nandrolone and testosterone. By combining innovative sensor design with advanced calibration methods, the study paves the way for improved steroid monitoring in sports, healthcare, and pharmaceutical industries. In [34] a cutting-edge graphene-based THz sensor is designed for accurate refractive index sensing and material characterization. Its tunability, high sensitivity, and ability to operate in the THz frequency range make it a promising tool for various scientific and industrial applications, particularly in material science, biomedical engineering, and chemical analysis. A highly sensitive refractive index sensor based on a graphene ring metasurface is introduced in [35]. By combining the advantages of graphene with the functionality of metasurfaces, the sensor offers excellent sensitivity, tunability, and versatility. It has significant potential for applications in bio-sensing, chemical analysis, and material characterization, particularly in the THz frequency range. This work represents a substantial contribution to the development of next-generation optical sensors.

This manuscript introduces a disk-shaped graphene-based absorber. The suggested structure is then modeled using the transmission line method (TLM), and the results of the simulation of the full-wave are compared with those from the theory of TLM to validate the precision of the full-wave simulation. In the next step of the article, to check the functionality of the refractive index sensor of the proposed structure, an analyte layer (substance under test) is placed on the proposed absorber, and by changing the refractive index of the analyte material, the absorption curve of the structure is checked, and the sensor parameters of this structure are obtained. In the last step, to improve the sensor parameters of the proposed structure, we create a pyramidal air hole in the dielectric layer. The proposed structure is highly suitable for the early detection like cancer and influenza. A simulation of the full wave of this structure was performed using CST software, and the coding was done to get the theoretical parameters of the transmission line using MATLAB software. The method of solving this structure is using FDTD with CST software.

II. ABSORBER THEORY AND DESIGN

The planned absorber structure, as shown in Fig. 1, comprises three layers: the bottom layer is gold with a conductivity of 4.56×10^7 S/m, the middle layer is SiO_2 with a relative permittivity of 2.25, and the upper layer is a disc-shaped graphene layer.

The dielectric substrate, labeled T1 in Fig. 1, has a thickness of 3.7 μm, while the layer of gold at the end has a thickness of 0.2 μm. Also, in this structure $P_x = P_y = 4.4\ \mu m$. The disc radius is $1.8\ \mu m$. The presence of a graphene layer in graphene-based THz absorber structures is due to this

material's unique properties. Graphene has high electrical conductivity and the ability to adjust its electronic properties through the application of an electric field or chemical changes. These features allow graphene to interact strongly with electromagnetic waves in the THz range and improve the absorption of these waves. Also, the very low thickness of graphene (a single atomic layer) helps to design very thin and light THz absorbers. The tunability of graphene allows engineers to create absorbers with controllable spectral response, which is useful for applications as diverse as optical sensors, imaging, and telecommunications. For this reason, the layer of graphene forms the main part of these absorbers' structures and helps to increase their efficiency and accuracy. In THz absorbers, the gold layer acts as a mirror or reflective layer that reduces the reflection of THz waves and traps the waves in the absorber structure. This feature causes the wave energy to be absorbed in graphene and the absorber efficiency increases.

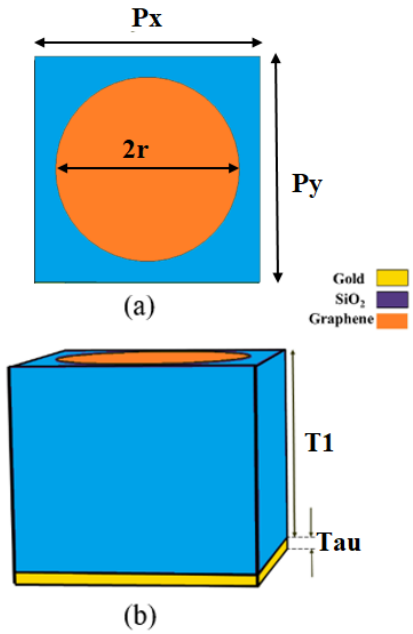

Fig. 1. (a) The top view of the planned perfect THz absorber (b) Side view.

When the THz wave hits a graphene-based absorber structure, several physical processes occur simultaneously, which ultimately lead to the absorption of the wave energy by the structure. The THz wave collides with an electrical (E) and magnetical (H) field to the upper surface of the structure, which consists of a graphene layer. This collision excites free electrons in graphene. Due to having free electrons and high conductivity, graphene strongly interacts with the THz wave electric field.

This interaction causes surface plasmon polariton (SPP) oscillations in the graphene layer. SPP oscillations are a collective movement of electrons on the surface of graphene that occurs at certain frequencies of THz. Due to the geometric pattern design (disk shapes) on the graphene surface, the SPP oscillations are resonantly amplified. This resonance enhances the accumulation of the electric field in particular areas of the structure, which results in enhanced absorption of THz wave energy by graphene. A portion of the THz wave that is not absorbed by the graphene passes through the SiO_2 layer and reaches the underlying gold layer. The gold layer serves as a highly effective reflector, bouncing the wave back. This reflection causes the wave to return to the graphene layer and pass through it once more. This repeated cycle of reflection and passage increases the probability of wave absorption. Each time a wave passes through the graphene and interacts with its electrons, a fraction of the wave's power is changed into heat. This power conversion constitutes the absorption process. In other words, the electromagnetic energy of the THz wave is converted into thermal energy, ultimately manifesting as energy loss within the structure. The design of the structure is such that the wave reflection is minimized and most of the wave energy is confined and absorbed within the proposed structure. The curve of absorption of the planned absorber is shown in Fig. 2. It illustrates that the peak of absorption at a frequency of 4.26 THz reaches 99.99%.

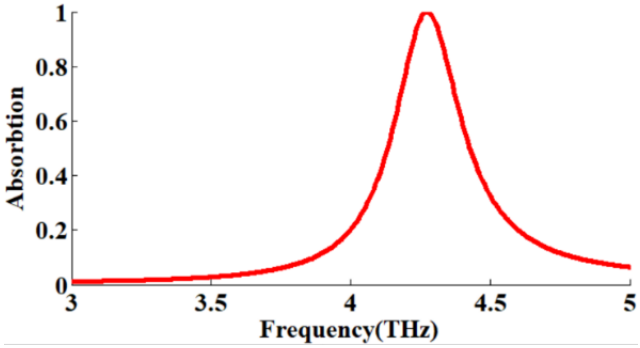

Fig. 2. The absorption spectrum of the proposed absorber.

To validate the simulation, we use the model of TLM for the suggested absorber. In this method, the graphene layer placed on the proposed absorber acts as a series resonator in the TLM. Graphene can stimulate SPP oscillations in response to electromagnetic waves. These collective oscillations of electrons on the graphene surface can be modeled as a resonator, where the plasmonic currents are amplified at a specific frequency. This resonant behavior is similar to a series resonator circuit in which the inductor and capacitor are arranged in series to reach resonance at a specific frequency. The gold layer at the end serves as a short circuit, while the dielectric layer is represented as a transmission line. Fig. 3 shows the TLM of the proposed structure. Also, the step-by-step Process of using the TLM theory is given in Fig. 4.

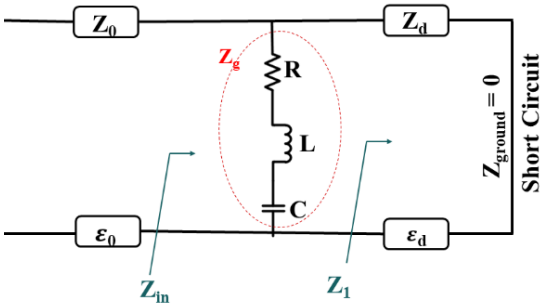

Fig. 3. Transmission line model of the planned structure.

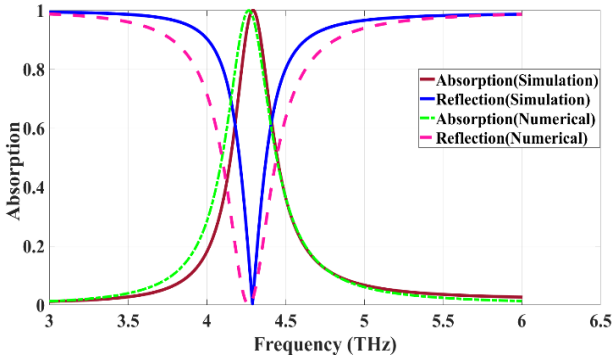

Fig. 4. The step-by-step stages of using the transmission line theory.

The design theory for the suggested absorber relies on the circuit model's validity, as outlined in recent studies [37–39]. Specifically, Ref. [39] models the entire array of graphene disks using the RLC circuit model, with each component defined as follows:

$$Y_G = \frac{\pi^2}{P^2}\left(\sigma_s{}^{-1} + \frac{q_{11}}{j\omega\varepsilon_{eff}}\right)^{-1}\frac{S_1{}^2}{K_1{}^2} = \frac{1}{R_1 + j\omega L_1 + \frac{1}{j\omega c_1}} = \frac{1}{Zg} \quad (1)$$

$$R_1 = \frac{h^2}{e^2 E_f \tau}\frac{K_1 P^2}{\pi S_1{}^2} \quad (2)$$

$$L_1 = \frac{h^2}{e^2 E_f}\frac{K_1 P^2}{\pi S_1{}^2} \quad (3)$$

$$C_1 = \frac{\varepsilon_{eff}}{q_{11}}\frac{\pi s_1^2}{K_1 P^2} \quad (4)$$

$$Z_1 = jZ_d tan(E_2) \quad (5)$$

$$E_2 = \beta_2 L = \beta_2 T1 \quad (6)$$

$$\beta_2 = 2\pi f\sqrt{\varepsilon_0 \varepsilon r \mu_0} \quad (7)$$

$$Z_d = \sqrt{\frac{\mu_0}{\varepsilon_0 \varepsilon r}} \quad (8)$$

$$Zin = \frac{Z_1 Z_g}{Z_1 + Z_g} \quad (9)$$

$$\Gamma = \frac{\mathrm{Re}\,(Z_{in}) - Z_0}{\mathrm{Re}\,(Z_{in}) + Z_0} \quad (10)$$

Where S_1=0.6087R and K_1=1.2937 are determined for the eigenvalue of the first, q_{11}signifies the eigenvalue of the first for the disk-shaped graphene. Here, σ_s represents the conductivity of the surface, and E_f denotes the level of Fermi energy, defined as E_f=eμ_c. The effective dielectric constant ε_{eff} is determined by $\varepsilon_{eff} = \frac{n_1{}^2 + n_2{}^2}{2}$ where n_1 and n_2 are the dielectric materials' refractive indices on the top and bottom layers of the graphene. In these equations, E_2 is the electrical length of the transmission line, β_2 Phase constant or wave number (related to propagation characteristics of the line), and L is the length of the transmission line. Fig. 5 illustrates a comparison between the full-wave simulation results and the model of the transmission line. It is evident that the simulation results align well with those obtained from the theory of TLM, and this indicates the validity of the proposed absorber performance.

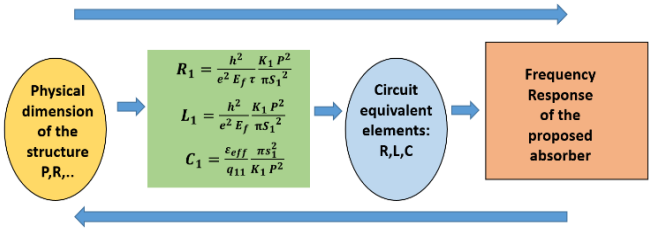

Fig. 5. Comparison of full wave simulation and transmission line model results.

III. REFACTIVE INDEX SENSOR

As observed from the results of the designed absorber, this structure has an absorption performance of 99.99% at the frequency of 4.26 THz, and at this frequency, it shows an excellent absorption performance, and this absorber can be used for the performance of the sensor of the refractive index. For this purpose, we put an analyte substance (substance under test) on the proposed absorber and change the refractive index of this substance. The absorption curve of this proposed structure shifts with the change of the refractive index of the analyte material, which indicates the sensor performance of the proposed structure. Fig. 6, shows the suggested sensor absorption curve for different refractive index values of the analyte.

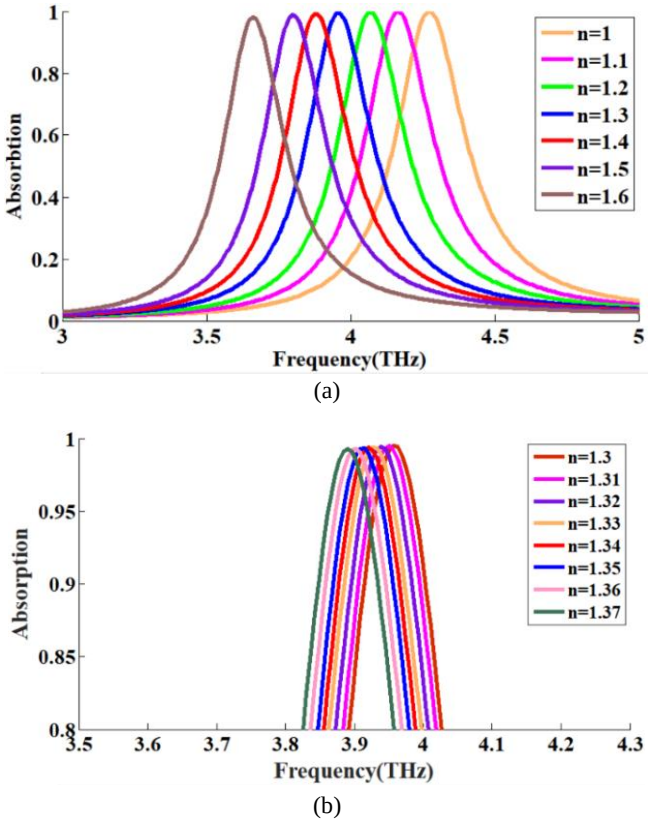

Fig. 6. Absorption curve of the suggested sensor for various values of the analyte refractive index.

Graphene-based refractive index sensors in the THz have several main parameters that are very important to evaluate their performance. These parameters include the following:

Sensitivity: The sensitivity responds to changes in the environment's refractive index in which the sensor is located and is expressed as a change in the resonance frequency or a change in absorption intensity per unit change in the refractive index.

Quality Factor: The quality factor expresses the relation of

the resonance frequency to the resonance bandwidth (FWHM). The higher quality factor indicates a narrower resonance peak and a more accurate resonance frequency.

FOM: The (Figure of Merit) quantifies the sensor's overall effectiveness, which is defined as the ratio of sensitivity to resonance bandwidth. In other words, FOM = Sensitivity / FWHM.

The higher the sensitivity, the more accurately a sensor can detect smaller changes in refractive index. A higher quality factor usually means increased sensor accuracy and reduced interference with noisy signals. A higher FOM indicates a sensor's better performance in detecting refractive index changes with high accuracy. The proposed sensor performance parameters are presented in Table I.

TABLE I
Sensor Characteristics at Different Refractive Index

Refractive index	RPF	FWHM [THz]	Sensitivity [THz/RIU]	FOM	Q-factor
1	4.275	0.294	-	-	14.54
1.1	4.167	0.288	0.96	3.33	14.46
1.2	4.065	0.282	1.08	3.82	14.41
1.3	3.957	0.276	1.08	3.91	14.33
1.4	3.879	0.27	0.72	2.66	14.36
1.5	3.801	0.264	0.9	3.4	14.39
1.6	3.663	0.253	1.32	5.2	14.47

To enhance the proposed refractive index sensor performance, we created two pyramidal holes at the end of the suggested sensor structure. The improved refractive index sensor is presented in Fig. 7. As shown in this figure, the pale pink color is the analyte method, which is placed on the designed absorber. The empty pyramid holes at the end of the substrate are also clearly seen in this figure. One of the challenges related to this structure is the steps related to constructing and producing these absorbers. The fabrication of the graphene-based terahertz absorber begins with cleaning a silicon wafer substrate using piranha solution or RCA methods to ensure a contaminant-free surface for subsequent layers. A 3.7 μm thick dielectric layer (e.g., SiO_2) is deposited on the substrate using plasma-enhanced chemical vapor deposition (PECVD) or thermal oxidation, followed by annealing to enhance its structural properties. A 0.2 μm thick gold layer is then deposited on the dielectric layer using electron beam evaporation or sputtering, with an optional adhesion layer (e.g., chromium or titanium) to improve bonding.

Next, graphene is synthesized via chemical vapor deposition (CVD) on a metal catalyst (e.g., copper) and transferred onto the gold layer using a PMMA-assisted wet transfer method. The metal catalyst is etched away, and the PMMA-graphene film is transferred onto the gold surface, followed by PMMA removal with acetone. The graphene is patterned into disc shapes with a radius of 0.9 μm using electron beam lithography (EBL). A positive resist is applied, exposed to an electron beam, and developed, followed by oxygen plasma etching to remove unwanted graphene. Finally, the remaining resist is stripped using acetone.

Post-fabrication, the structure is inspected using scanning electron microscopy (SEM) for dimensional accuracy and Raman spectroscopy to confirm graphene quality. Optional annealing may be performed to eliminate defects and improve performance. This process ensures precise fabrication of the terahertz absorber with high performance and structural integrity [40-43].

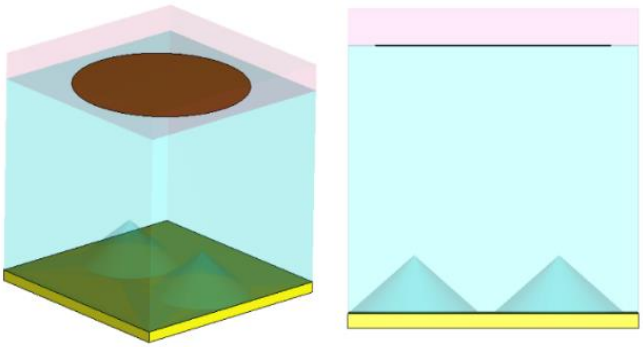

Fig. 7. The modified refractive index sensor structure.

The absorption curve of the improved sensor is depicted in Fig. 8. As evident in this figure, the sensitivity of the sensor is improved by creating a pyramid under the substrate, and this condition can be observed by observing the distance of the two frequencies for two different refractive indices.

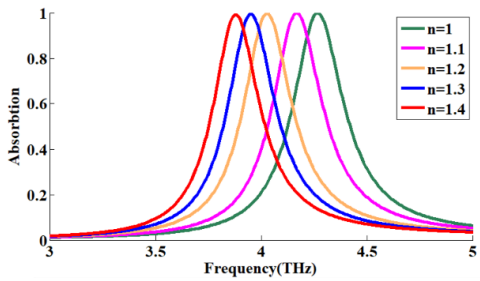

Fig. 8. The absorption curve of the modified refractive index sensor.

To check the functional mechanism of the suggested sensor, Fig. 9 demonstrates the electric field distribution curve. This figure displays the electrical field distribution from both the top and side views for each case.

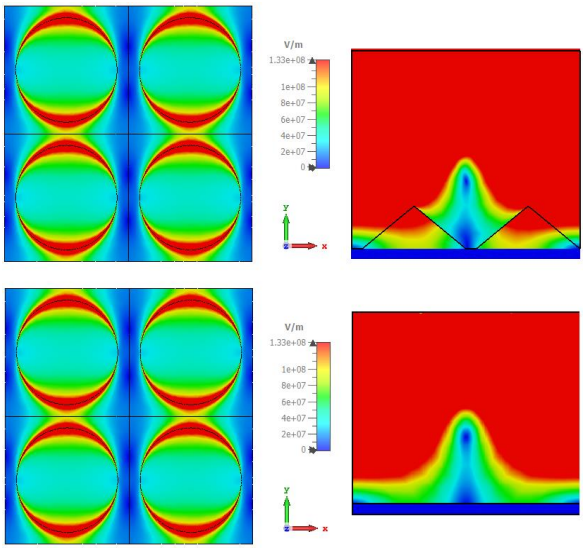

Fig. 9. The electric field distribution of both refractive index sensors.

Table II provides the improved sensor parameters. As shown in this table, the quality coefficient of the proposed absorber has improved from 14 to 22. The reason for this is that with the creation of a pyramid, the electric field distribution has changed compared to the state without a pyramid, and this change is caused by several factors.

TABLE II
Absorption Characteristics of the Modified Sensor at Various Refractive Index

Refractive index	RPF	FWHM [THz]	Sensitivity [THz/RIU]	FOM	Quality factor
1	4.26	0.192	-	-	22.18
1.1	4.173	0.186	1.02	5.48	22.43
1.2	4.035	0.189	1.32	6.98	21.34
1.3	3.951	0.174	0.78	4.48	22.7
1.4	3.873	0.174	0.78	4.48	22.25

Due to their specific geometry, pyramids can concentrate the electric field at certain points. Because the tips of the pyramids are sharp and thin, the electric fields are naturally amplified at these points. This phenomenon is known as "Field Enhancement". When the electrical field is focused in an area, the absorption of the energy by the material in that area increases. Also, uneven pyramidal surfaces cause multiple scattering of electromagnetic waves. These scatterings cause the incoming waves to enter the absorbing structure and take different paths, which increases the chance of absorbing more energy. In other words, the pyramids increase the difference paths for the waves inside the absorber, which, as an outcome, increases the amount of energy absorption. This sensor can be a suitable candidate for diagnosing diseases such as malaria and influenza, and can have many applications in the medical industry.

The comparison of the performance of this sensor with the sensors of previous researchers is given in Table III**.**

Comparing the results obtained from this design and similar works indicates that the proposed sensor can be a suitable candidate for diagnosing diseases such as malaria and influenza and can have many applications in the medical industry.

IV. CONCLUSIONS

This study successfully demonstrates the design and optimization of a graphene-based refractive index sensor for THz applications, emphasizing the importance of pyramidal air holes in the dielectric layer for enhanced performance. The introduction of pyramidal holes significantly improved the sensor's sensitivity and quality factor, making it a promising tool for detecting small changes in the refractive index. The full-wave simulations and transmission line method validations confirm the effectiveness of the suggested design, showing strong agreement between theoretical and simulated results. With its high absorption rate (99.99% at 4.26 THz) and enhanced sensitivity from 14 to 23, the proposed sensor holds great potential for use in medical diagnostics and other fields requiring precise refractive index measurements.

TABLE III
Comparison Table Between Refractive Index Sensor Characteristics Described in the Recent Research and the Planned Sensor

Ref.	Year	Frequency Range[THz]	Sensitivity [THz/RIU]	FOM	Q-factor
[44]	2012	0.2–0.3	0.225	NR	NR
[45]	2013	2.5–5	0.13	1.04	NR
[46]	2013	0–1.2	0.261	NR	NR
[47]	2014	0.4–1	0.163	2.67	7.189
[48]	2014	0.4–3	0.261	NR	NR
[49]	2015	2–14	1.9082	6.5662	54&59
[50]	2016	0–3.2	1.6	14.55	NR
[51]	2016	0.5–1	0.5	NR	NR
[52]	2016	0–3	0.457	3.1	NR
[53]	2017	2.5–4.5	1.966	19.86	87.32
[54]	2017	0.4–2.8	0.968	1.2	NR
[55]	2017	0.5–1.77	0.638	NR	NR
[56]	2017	0.1–0.9	0.127	46.8	NR
[57]	2018	1–6.5	0.36	3.64	19.2
[58]	2018	0.3–1.2	0.105	7.501	58
[59]	2018	1.5–2.5	0.36	431	120
[60]	2019	2–5	1.75	NR	347
[61]	2019	0.2–1.4	0.49	23	9.4
[62]	2019	1–2.2	0.3	NR	NR
[63]	2019	1.1–2.1	0.54	2.86	NR
[64]	2019	2.2–3.2	0.2695	5.39	48.3
[65]	2019	3.82	0.16	62.81	1432
[66]	2019	0.6–1.2	0.085	NR	NR
[67]	2019	1.5–3	0.3	2.94	22.05
[68]	2019	0.8–1.2	0.28	NR	NR
[69]	2020	2.1–6.25	1.57	11.75 &24.5	40.1 &80
[70]	2020	0.4–2.5	0.5	15	NR
[71]	2020	0.1–1.9	0.28	8.54	30.5
[72]	2021	1–2	1.84	NR	277.8
[73]	2022	2.5–4.5	1.6498	NR	11.33
[74]	2023	6.29–7.512	2.538	8.73	23.4
[75]	2023	1.3	0.473	16.9	NR
[76]	2024	3.24	0.726	2.69	NR
This work	2024	4.26	1.32	6.98	22.25

NR: not reported

V. REFERENCES

[1] Pawar, A. Y., Sonawane, D. D., Erande, K. B., & Derle, D. V. (2013). THz technology and its applications. *Drug Invention Today*, *5*(2), 157-163.

[2] Lu, W., Zhao, W., Ma, C., Yi, Z., Zeng, Q., Wu, P., ... & Jiang, P. (2024). A simulation work on a thermally tunable and highly sensitive THz smart window device with dual-band absorption and wide-ranging transmission based on VO_2 phase-change material. *Optics & Laser Technology*, *178*, 111210.

[3] Khani, S., Danaie, M., Rezaei, P., Shahzadi, A. (2020) Compact ultra-wide upper stopband microstrip dual-band BPF using tapered and octagonal loop resonators. *Frequenz*, 74(1-2), 61-71.

[4] Uddin, J. (Ed.). (2017). *THz Spectroscopy: A Cutting Edge Technology*. BoD–Books on Demand.

[5] Kiani, S., Rezaei, P., Fakhr, M. (2023) Investigation of microwave resonant sensors for use in detecting changes of noninvasive blood glucose concentration, John Wiley and Sons, 45, 1055-1064.

[6] Babu, K. V., & Sree, G. N. J. (2023). Design and circuit analysis approach of graphene-based compact metamaterial-absorber for THz

range applications. *Optical and Quantum Electronics*, *55*(9), 769.

[7] Chen, Z., Cai, P., Wen, Q., Chen, H., Tang, Y., Yi, Z., ... & Yi, Y. (2023). Graphene multi-frequency broadband and ultra-broadband THz absorber based on surface plasmon resonance. *Electronics*, *12*(12), 2655.

[8] Ri, K. J., Kim, J. S., Kim, J. H., & Ri, C. H. (2023). Tunable triple-broadband THz metamaterial absorber using a single VO2 circular ring. *Optics Communications*, *542*, 129573.

[9] Zheng, C., Li, J., Liu, L., Li, J., Yue, Z., Hao, X., ... & Yao, J. (2022). Optically tunable THz metasurface absorber. *Annalen der Physik*, *534*(5), 2200007.

[10] Alipour, A.H., Khani, S., Ashoorirad, M., Baghbani, R. (2023). Trapped multimodal resonance in magnetic field enhancement and sensitive THz plasmon sensor for toxic materials accusation. *IEEE Sensor Journal*, 23(13), 14057-14066.

[11] Khatami, S. A., Rezaei, P., & Zamzam, P. (2022). Quad-band metal-dielectric-metal perfect absorber to selective sensing application. *Optical and Quantum Electronics*, *54*(10), 638.

[12] Fakharian, M.M. (2024) Design of a terahertz metasurface absorber based on machine learning technique, *Tabriz Journal of Electrical Engineering*, 54(3), 291-299.

[13] Wang, J., Qin, X., Zhao, Q., Duan, G., & Wang, B. X. (2024, February). Five-band tunable THz metamaterial absorber using two sets of different-sized graphene-based copper-coin-like resonators. *MDPI Photonics*, vol. 11, no. 3, p. 225.

[14] Du, C., Zhou, D., Guo, H. H., Pang, Y. Q., Shi, H. Y., Liu, W. F., ... & Xu, Z. (2020). An ultra-broadband THz metamaterial coherent absorber using multilayer electric ring resonator structures based on anti-reflection coating. *Nanoscale*, *12*(17), 9769-9775.

[15] Khani, S., Hayati, M. (2021) An ultra-high sensitive plasmonic refractive index sensor using an elliptical resonator and MIM waveguide. *Superlattices and Microstructures*, 156, 106970

[16] Hadipour, S., Rezaei, P., & Norouzi-Razani, A. (2024). Multi-band square-shaped polarization-insensitive graphene-based perfect absorber. *Optical and Quantum Electronics*, *56*(3), 471.

[17] Weiss, N. O., Zhou, H., Liao, L., Liu, Y., Jiang, S., Huang, Y., & Duan, X. (2012). Graphene: an emerging electronic material. *Advanced materials*, *24*(43), 5782-5825.

[18] Rhee, K.Y. (2020). Electronic and thermal properties of graphene. *Nanomaterials*, *10*(5), 926.

[19] Khodadadi, B., Rezaei, P., Hadipour, S. (2025). Dual-band polarization-independent maze-shaped absorber based on graphene for terahertz biomedical sensing. *Optics Express*, 33(1), 545227.

[20] Khani, S., Hayati, M. (2022). Optical biosensors using plasmonic and photonic crystal band-gap structures for the detection of basal cell cancer, *Scientific Reports*, 12(1), 5246.

[21] Song, Y., Deng, X. H., Zhang, P., Guo, F., & Qin, K. (2024). Graphene-Based Metamaterial Absorber with Perfect Multi-band Absorption. *Journal of Electronic Materials*, 1-10.

[22] Korani, N., Mohammadi, S., et al. (2024). A tunable graphene dual mode absorber for efficient THz radiation absorption and sensing applications. *Diamond and Related Materials*, 111554.

[23] Lai, R., Chen, H., Zhou, Z., Yi, Z., Tang, B., Chen, J., ... & Sun, T. (2023). Design of a penta-band graphene-based THz metamaterial absorber with fine sensing performance. *Micromachines*, *14*(9), 1802.

[24] Zamzam, P., Rezaei, P., Khatami, S.A., & Appasani, B. (2025). Super perfect polarization-insensitive graphene disk terahertz absorber for breast cancer detection using deep learning. *Optics & Laser Technology*, 183, 112246.

[25] Khani, S., Hayati, M. (2022). Optical sensing in single-mode filters base on surface plasmon H-shaped cavities, *Optics Communications*, 505, 127534.

[26] Mohsen Daraei, O., Rezaei, P., Zamzam, P., et al. (2024). Single/multi-band graphene-based disk THz absorbers with single graphene layer: Conceptual design. *Optical and Quantum Electronics*, 56(11),1844.

[27] Rangasamy, S., Khansadurai, A. M., Venugopal, G., & Udayakumar, A. K. (2023). Graphene-based O-shaped metamaterial absorber design with broad response for solar energy absorption. *Optical and Quantum Electronics*, *55*(1), 90.

[28] Zamzam, P., & Rezaei, P. (2022). Renovation of dual-band to quad-band polarization-insensitive and wide incident angle perfect absorber based on the extra graphene layer. *Micro Nanostruct.*, *168*, 207261.

[29] Alizadeh, S., Zareian-Jahromi, E., & Mashayekhi, V. (2022). A tunable graphene-based refractive index sensor for THz bio-sensing applications. *Optical and Quantum Electronics*, *54*, 1-13.

[30] Patel, S. K., Solanki, N., Charola, S., Parmar, J., Zakaria, R., Faragallah, O. S., ... & Rashed, A. N. Z. (2022). Graphene-based highly sensitive refractive index sensor using double split ring resonator metasurface. *Optical and Quantum Electronics*, *54*(3), 203.

[31] Nickpay, M. R., Danaie, M., & Shahzadi, A. (2022). Design of a graphene-based multi-band metamaterial perfect absorber in THz frequency region for refractive index sensing. *Physica E: Low-dimensional Systems and Nanostructures*, *138*, 115114.

[32] Rezagholizadeh, E., Biabanifard, M., & Borzooei, S. (2020). Analytical design of tunable THz refractive index sensor for TE and TM modes using graphene disks. *J. Physics D: Appl. Phys.*, *53*(29), 295107.

[33] Jalalvand, A.R., Rashidi, Z., Khajenoori, M. (2023) Sensitive and selective simultaneous biosensing of nandrolone and testosterone as two anabolic steroids by a novel biosensor assisted by second-order calibration. *Steroids*, 189, 109138.

[34] Veeraselvam, A., Mohammed, G. N. A., Savarimuthu, K., Anguera, J., Paul, J. C., & Krishnan, R. K. (2021). Refractive index-based THz sensor using graphene for material characterization. *Sensors*, *21*(23), 8151.

[35] Rastgordani, A., & Kashani, Z. G. (2020). High-sensitive refractive index sensors based on graphene ring metasurface. *Optics Communications*, *474*, 126164.

[36] Li, C., & Wu, Q. (2024). Graphene-based tunable high-sensitivity metasurface refractive index sensor. *Plasmonics*, 1-12.

[37] Biabanifard, M., & Abrishamian, M. S. (2018). Circuit modeling of tunable THz graphene absorber. Optik, 158, 842-849.

[38] Biabanifard, M., & Abrishamian, M. S. (2018). Multi-band circuit model of tunable THz absorber based on graphene sheet and ribbons. *AEU-Int. J. Electron. and Commun.*, *95*, 256-263.

[39] Barzegar-Parizi, S., Rejaei, B., & Khavasi, A. (2015). Analytical circuit model for periodic arrays of graphene disks. *IEEE Journal of Quantum Electronics*, *51*(9), 1-7.

[40] Ferrari, A.C., Basko, D.M. (2013). Raman spectroscopy is a versatile tool for studying the properties of graphene. *Nature Nanotechnology*, 8(4), 235-246.

[41] Novoselov, K.S., et al. (2004). Electric field effect in atomically thin carbon films. *Science*, 306, 5696, 666-669.

[42] Smith, D. R., Pendry, J.B. (2006). Homogenization of metamaterials by field averaging. *JOSA B* 23(3), 391-403.

[43] Yan, D., et al. Graphene-assisted narrow bandwidth dual-band tunable terahertz metamaterial absorber. *Frontiers in Physics* 8 (2020): 306.

[44] V. Astley, K.S. Reichel, J. Jones, R. Mendis, D.M. Mittleman, THz multichannel microfluidic sensor based on parallel-plate waveguide resonance cavities, Appl. Phys. Lett. 100 (23) (2012), 231108.

[45] C.Y. Chen, Y.H. Yang, T.J. Yen, Unveiling the electromagnetic responses of fourfold symmetric metamaterials and their THz sensing capability, Appl. Phys. Express. 6 (2) (2013), 022002.

[46] B. You, J.Y. Lu, T.A. Liu, J.L. Peng, Hybrid THz plasmonic waveguide for sensing applications, Opt. Express 21 (18) (2013) 21087–21096.

[47] L. Cong, R. Singh, Sensing with THz metamaterial absorbers, arXiv preprint arXiv: (2014) 1408.3711.

[48] F. Fan, et al., THz refractive index sensing based on photonic column array, IEEE Photon. Technol. Lett. 27 (5) (2014) 478–481.

[49] Y. Zhang, T. Li, B. Zeng, H. Zhang, H. Lv, X. Huang, W. Zhang, A.K. Azad, A graphene-based tunable THz sensor with double Fano resonances, Nanoscale 7 (29) (2015) 12682–12688.

[50] B.X. Wang, G.Z. Wang, T. Sang, Simple design of novel triple-band THz metamaterial absorber for sensing application, J. Phys. Appl. Phys. 49 (16) (2016),165307.

[51] A. Soltani, H. Neshasteh, A. Mataji-Kojouri, N. Born, E. CastroCamus, M. Shahabadi, M. Koch, Highly sensitive THz dielectric sensor for smallvolume liquid samples, Appl. Phys. Lett. 108 (19) (2016), 191105.

[52] X. Hu, et al., Metamaterial absorber integrated microfluidic THz sensors, Laser Photon. Rev. 10 (6) (2016) 962–969.

[53] X. Chen, W. Fan, Ultrasensitive THz metamaterial sensor based on spoof surface plasmon, Sci. Rep. 7 (2017) 2092.

[54] Y. Xin, L. Lan-Ju, D. Xin, Y. Jian-Quan, Solid analyte and aqueous solutions sensing based on a flexible THz dual-band metamaterial absorber, Opt. Eng. 56 (2) (2017) 1–6.

[55] W. Zhang et al., Ultrasensitive dual-band THz sensing with metamaterial perfect absorber, IEEE MTT-S Int. Microw. Workshop Adv. Mater. Process. for RF THz Appl. 17488695 (2017) 1-3.

[56] W. Wang, et al., Experimental demonstration of an ultra-flexible metamaterial absorber and its application in sensing, J. Phys. D: Appl. Phys. 50 (13) (2017), 135108.

[57] P.R. Tang, J. Li, L.H. Du, Q. Liu, Q.X. Peng, J.H. Zhao, B. Zhu, Z.R. Li, L.G. Zhu, Ultrasensitive specific THz sensor based on tunable plasmon-induced transparency of a graphene micro-ribbon array structure, Opt. Express 26 (23) (2018) 30655–30666.

[58] Q. Xie, G.X. Dong, B.X. Wang, et al., High-Q fano resonance in THz frequency based on an asymmetric metamaterial resonator, Nanoscale

Res. Lett. 13 (294) (2018).
[59] M. Janneh, A. De Marcellis, E. Palange, A.T. Tenggara, D. Byun, Design of a metasurface-based dual-band THz perfect absorber with very high Q-factors for sensing applications, Opt. Commun. 416 (2018) 152–159.
[60] S. Niknam, M. Yazdi, S. Behboudi Amlashi, Enhanced ultra-sensitive metamaterial resonance sensor based on double corrugated metal stripe for THz sensing, Sci. Rep. 9 (2019) 7516.
[61] F. Lan, F. Luo, P. Mazumder, Z. Yang, L. Meng, Z. Bao, J. Zhou, Y. Zhang, S. Liang, Z. Shi, A. Rauf Khan, Z. Zhang, L. Wang, J. Yin, H. Zeng, Dual-band refractometric THz biosensing with intense wave-matter-overlap microfluidic channel, Biomed. Opt. Express 10 (8) (2019) 3789–3799.
[62] Z. Vafapour, W. Troy, A. Rashidi, Colon cancer detection by designing and analytical evaluation of a water-based THz metamaterial perfect absorber, IEEE Sens. J. 21 (17) (2021) 19307–19313.
[63] A. Keshavarz, Z. Vafapour, Sensing avian influenza viruses using THz metamaterial reflector, IEEE Sens. J. 19 (13) (2019) 5161–5166.
[64] S. Hu, D. Liu, H. Yang, H. Wang, Y. Wang, Staggered H-shaped metamaterial based on electromagnetically induced transparency effect and its refractive index sensing performance, Opt. Commun. 450 (2019) 202–207.
[65] F.G. Vanani, A. Fardoost, R. Safian, Design of double ring labelfree THz sensor, IEEE Sens. J. 19 (4) (2019) 1293–1298.
[66] L.S. Li, F. Hu, Z. Chen, W. Zhang, J. Han, Metamaterial THz sensor for measuring thermal-induced denaturation temperature of insulin, IEEE Sensor J. 20 (4) (2019) 1821–1828.
[67] A.S. Saadeldin, et al., Highly sensitive THz metamaterial sensor, IEEE Sens. J.19 (18) (2019) 7993–7999.
[68] Y.K. Srivastava, et al., THz sensing of 7 nm dielectric film with bound states in the continuum metasurfaces, Appl. Phys. Lett. 115 (15) (2019), 151105.
[69] E. Rezagholizadeh, M. Biabanifard, S. Borzooei, Analytical design of tunable THz refractive index sensor for TE and TM modes using graphene disks, J. Phys. Appl. Phys. 53 (2020), 295107.
[70] Y. Wang, D. Zhu, Z. Cui, L. Yue, X. Zhang, L. Hou, K. Zhang, H. Hu, Properties and sensing performance of all-dielectric metasurface THz absorbers, IEEE Trans.THz Sci. Tech. 10 (6) (2020) 599–605.
[71] T. Chen, D. Zhang, F. Huang, Z. Li, F. Hu, Design of a THz metamaterial sensor based on split ring resonator nested square ring resonator, Mater. Res. Express 7 (9) (2020), 095802.
[72] X. Du, F. Yan, W. Wang, L. Zhang, Z. Bai, H. Zhou, Y. Hou, Thermally-stable graphene metamaterial absorber with excellent tunability for high-performance refractive index sensing in the THz band, Opt. Las. Tech. 144 (2021), 107409.
[73] M.Y. Azab, M.F.O. Hameed, A.M. Nasr, S.S.A. Obayya, Highly sensitive metamaterial biosensor for cancer early detection, IEEE Sens. J. 21 (6) (2021)7748–7755.
[74] Zamzam, P., Rezaei, P., Abdulkarim, Y. I., & Daraei, O. M. (2023). Graphene-based polarization-insensitive metamaterials with perfect absorption for THz biosensing applications: Analytical approach. *Optics & Laser Technology*, *163*, 109444.
[75] Barzegar-Parizi, S. (2023). Refractive index sensor with dual sensing bands based on an array of Jerusalem cross cavities to detect the hemoglobin concentrations. *Opt. Quantum Electron.*, *55*(1), 46.
[76] Khatami, S. A., Rezaei, P., & Danaie, M. (2024). High accuracy graphene-based refractive index sensor: Analytical approach. *Diamond and Related Materials*, *146*, 111225.